JOC The Journal of Organic Chemistry

Article

pubs.acs.org/joc

Pyreniporphyrins: Porphyrin Analogues That Incorporate a Polycyclic Aromatic Hydrocarbon Subunit within the Macrocyclic Framework

Ruixiao Gao, Deyaa I. AbuSalim, and Timothy D. Lash*

Department of Chemistry, Illinois State University, Normal, Illinois 61790-4160, United States

Supporting Information

ABSTRACT: The first examples of porphyrin analogues incorporating pyrene units are reported. Acid-catalyzed condensation of a pyrene dialdehyde with a tripyrrane, followed by oxidation with DDQ, afforded a polycyclic aromatic hydrocarbon (PAH)−porphyrin hybrid in 38% yield. Pyreniporphyrin proved to be devoid of global aromatic character, but upon protonation aromatic mono- and dicationic species were generated. In the proton NMR spectrum for the dication, the internal CH was shifted upfield to approximately +3 ppm. NICS calculations and ACID plots confirmed the diatropic nature of these structures. Pyreniporphyrin reacted with palladium(II) acetate to give excellent yields of a palladium(II) complex that showed weakly diatropic properties. Treatment of the pyrene dialdehyde with phenylmagnesium bromide generated a dicarbinol that reacted with excess pyrrole in the presence of boron trifluoride etherate to give a tripyrrane analogue. Lewis acid catalyzed ring closure with a thiophene dialcohol in 2% ethanol−dichloromethane afforded a tetraphenylthiapyreniporphyrin in 31% yield. This porphyrinoid was nonaromatic in the free-base form but showed significant diatropicity upon protonation. These results demonstrate that PAH−porphyrin hybrids are easily accessible, and this strategy may allow the incorporation of even larger aromatic subunits.

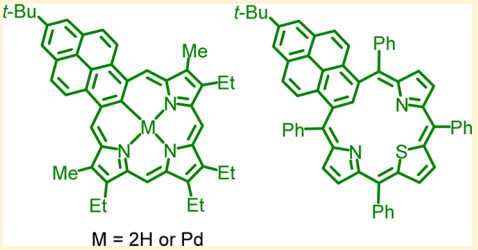

INTRODUCTION

Carbaporphyrinoid systems are porphyrin analogues in which one or more carbon atoms has been placed within the macrocyclic cavity.[1] These include true carbaporphyrins such as **1a** and **1b**,[2,3] azuliporphyrins **2**,[4] tropiporphyrins **3**,[5] N-confused porphyrins **4**,[6] and benziporphyrins **5**.[7] The properties of these species vary considerably, ranging from fully aromatic structures such as **1a**, **1b**, and **4** to nonaromatic benziporphyrins such as **5**.[1] Carbaporphyrinoids exhibit interesting reactivity, undergoing regioselective oxidation reactions[8,9] and readily generating organometallic derivatives.[10] Although the proton NMR spectra of benziporphyrins show no sign of global aromatic character, weak diatropicity manifests upon protonation.[11−13] In addition, electron-donating methoxy substituents imbue benziporphyrins with significant diatropic character,[14,15] and further modified structures can take on fully aromatic characteristics.[16,17] In order to further probe these intriguing properties, a related naphthalene-containing porphyrin analogue named naphthiporphyrin (**6**) was investigated.[17] It was hypothesized that the cross-conjugated benzene unit in **5** interferes with the overall aromaticity of the macrocycle and that this can only be overcome at the expense of losing the 6π electron arene aromaticity. As the resonance stabilization energy of the individual benzene rings in naphthalene are lower than for benzene itself, it was possible that naphthiporphyrin **6** could take on a degree of global diatropicity. However, the proton NMR spectrum for **6** showed no sign of macrocyclic aromaticity,[17] and this observation was confirmed by nucleus-independent chemical shift (NICS) calculations.[13] Protonation of naphthiporphyrin gave rise to a dication that exhibited some diatropic character, but this was only marginally greater than the shifts observed for the related benziporphyrin dication.[17]

Porphyrin-type systems that are associated with large aromatic subunits and related heterographene-like species have recently received considerable attention.[18] These include porphyrins with fused polycyclic aromatic units including naphthoporphyrins,[19] phenanthroporphyrins,[20] acenaphthoporphyrins,[21] anthracene-fused porphyrins,[22] fluoranthoporphyrins,[23] pyrene-fused porphyrins,[24] and corannulenoporphyrins.[25,26] An alternative approach is to introduce the polycyclic aromatic subunit as a component of the macrocyclic ring[27] as is the case for phenanthriporphyrin **7**[28] and related phenanthrisapphyrins.[29] The formation of hybrids between polycyclic aromatic hydrocarbons (PAHs) and porphyrins has not as yet been explored in any detail. We were interested in observing the effect of introducing a pyrene subunit within the porphyrinoid framework. Pyreniporphyrin **8** can be considered a modified benziporphyrin, and for the purposes of this study the numbering system used for benziporphyrins was retained for the new macrocyclic system. It was anticipated that the introduction of this conjugated tetracyclic subunit would further modify the aromatic and spectroscopic properties of the carbaporphyrinoid structure while retaining its ability to generate organometallic derivatives. Heterobenziporphyrins have also been reported recently,[30,31] and similarly modified structures such as 24-thiapyreniporphyrin **9** were also of

Received: April 8, 2017
Published: June 2, 2017

ACS Publications © 2017 American Chemical Society

DOI: 10.1021/acs.joc.7b00829
J. Org. Chem. 2017, 82, 6680−6688

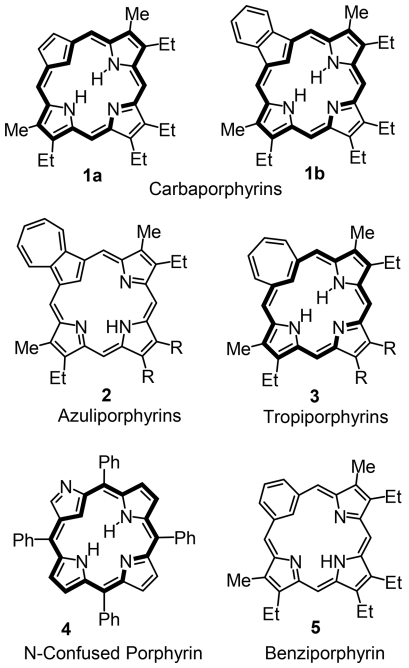

interest. In this paper, efficient routes to a pyreniporphyrin and a thiapyreniporphyrin are reported, and the properties of this new family of PAH−porphyrin hybrids has been explored.[32]

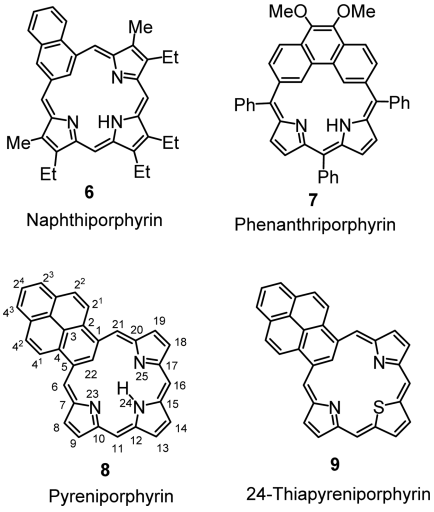

RESULTS AND DISCUSSION

The "3 + 1" variant on the MacDonald condensation has been widely used to prepare porphyrins and porphyrin analogues,[33] and this route is well suited for the synthesis of a pyreniporphyrin. In order to carry out syntheses of this type, appropriately substituted dialdehyde precursors are required. In fact, an example of a suitable pyrene dialdehyde **10** has previously been reported.[34] Friedel−Crafts alkylation of pyrene with *tert*-butyl chloride and aluminum chloride afforded 2-*tert*-butylpyrene (**11**), and subsequent bromination produced tribromo derivative **12** (Scheme 1).[34] In the original study,[34] **12** was treated with *tert*-butyllithium, but in our work this reagent was substituted with *n*-butyllithium. This was primarily due to safety considerations, as *tert*-butyllithium is highly pyrophoric, and comparable results were obtained when the metalated intermediate was treated with DMF and quenched with saturated ammonium chloride solution to produce the

Scheme 1

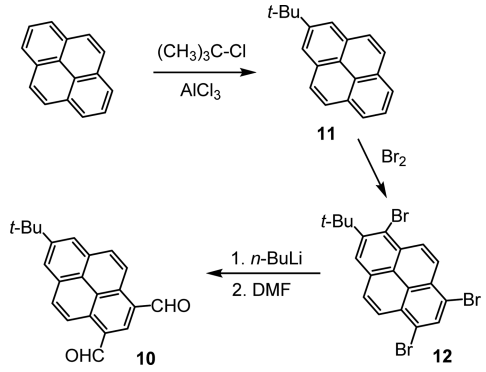

required dialdehyde **10**. In this chemistry, the *tert*-butyl moiety blocks the adjacent positions, which prevents the formation of the trialdehyde. The presence of the *tert*-butyl substituent directs the regioselectivity of this chemistry, but it is also valuable in its own right as this unit is likely to enhance the solubility of the resulting porphyrinoid products.

Tripyrrane **13** was treated with trifluoroacetic acid (TFA), the solution diluted with dichloromethane, and pyrene dialdehyde **10** was added in a single portion (Scheme 2).

Scheme 2

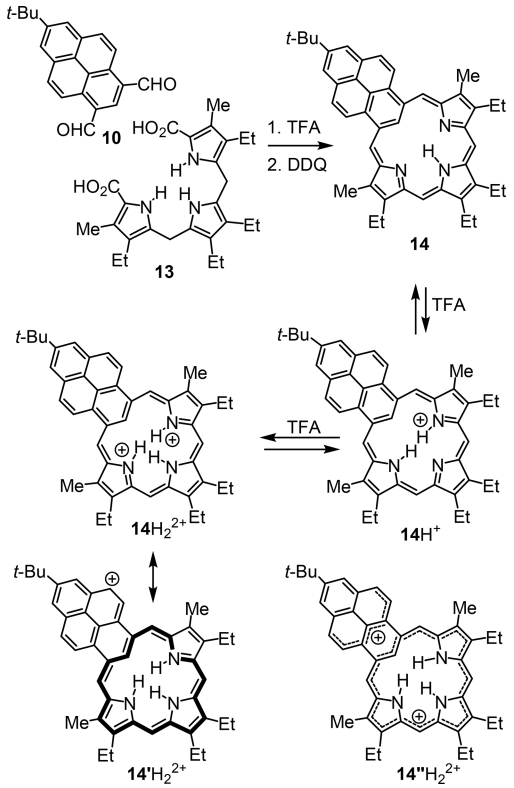

The mixture was stirred for 5 h under nitrogen and then oxidized with DDQ. Purification by column chromatography gave a deep green band, and subsequent recrystallization from chloroform−methanol afforded pyreniporphyrin **14** in 38% yield. The UV−vis spectrum for **14** gave rise to a series of moderate bands between 300 and 700 nm (Figure 1) that showed no resemblance to the spectra for true porphyrins, which have a characteristic Soret band and a series of smaller

DOI: 10.1021/acs.joc.7b00829
J. Org. Chem. 2017, 82, 6680−6688

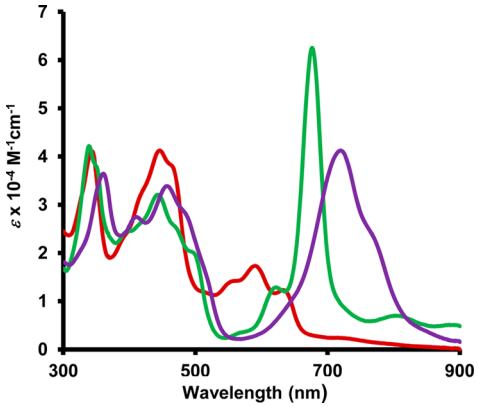

Figure 1. UV−vis spectra of pyreniporphyrin **14** in dichloromethane (free base, red line) with 1 equiv of TFA in dichloromethane (monocation $\mathbf{14}H^+$, green line) and with 100 equiv of TFA in dichloromethane (dication $\mathbf{14}H_2^{2+}$, purple line).

Q-bands. The proton NMR spectrum of **14** in $CDCl_3$ showed the external *meso*-protons as two 2H singlets at 6.49 and 8.31 ppm, values that are consistent with a nonaromatic porphyrinoid system (Figure 2). The 6,21-protons were shifted

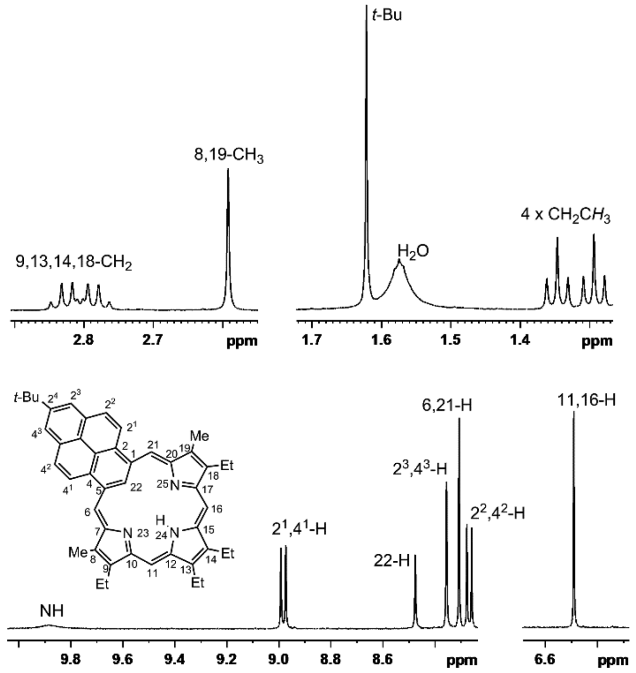

Figure 2. Partial 500 MHz proton NMR spectrum of pyreniporphyrin **14** in $CDCl_3$ showing the absence of a macrocyclic ring current.

relatively far downfield, but this is due to their proximity to the pyrene subunit. The internal CH and NH protons appeared at 8.47 and 9.88 ppm, respectively, again showing no sign of the upfield shifts associated with an aromatic macrocycle. Further information can be gleaned from the methyl resonances. In fully aromatic porphyrinoids, methyl substituents are shifted downfield due to their proximity to the aromatic ring current to approximately 3.5 ppm.[35] However, in the proton NMR spectrum for **14** the methyl groups produced a 6H singlet at 2.59 ppm. In the carbon-13 NMR spectrum, the *meso*-carbons appeared at 93.3 and 116.5 ppm, while the internal CH was identified at 119.3 ppm. Both the proton and carbon-13 NMR spectra confirm the presence of a plane of symmetry. The identity of **14** was confirmed by high-resolution ESI mass spectrometry.

Addition of 1 equiv of TFA to a solution of **14** in dichloromethane gave rise to a very different UV−vis spectrum that showed a strong absorption at 677 nm and weaker absorptions between 300 and 500 nm (Figure 1). This spectrum was attributed to the formation of monocation $\mathbf{14}H^+$ (Scheme 2). Further addition of TFA resulted in the formation of a new species that gave a broader band at 727 nm together with altered absorptions in the 300−500 nm region (Figure 1). This was ascribed to the production of dication $\mathbf{14}H_2^{2+}$. Dications derived from benziporphyrin **5** and naphthiporphyrin **6** exhibited significant diatropic character, and it was of interest to see whether this was also the case for pyreniporphyrin **14**. The proton NMR spectrum of $\mathbf{14}H_2^{2+}$ in TFA−$CDCl_3$ (Figure 3) showed the external *meso*-protons at

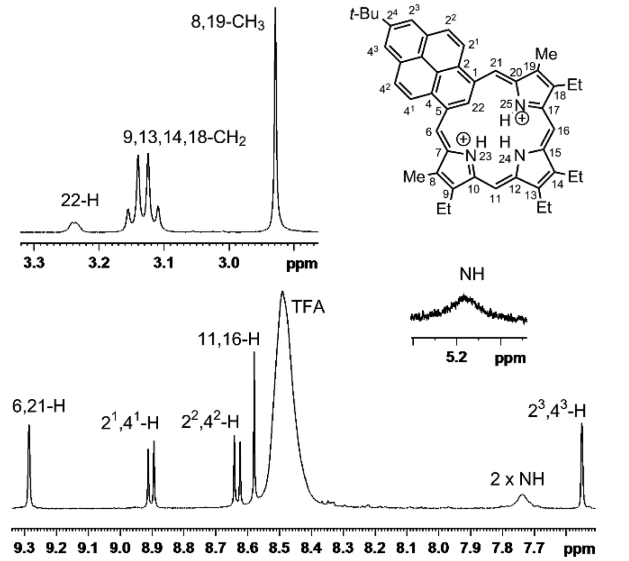

Figure 3. Partial 500 MHz proton NMR spectrum of pyreniporphyrin dication $\mathbf{14}H_2^{2+}$ in TFA−$CDCl_3$ demonstrating the presence of a significant global aromatic ring current.

7.65 and 9.37 ppm, values that are >1 ppm downfield from the corresponding resonances observed for the free base form. While this might arise in part from the presence of the positive charges, the result indicates the emergence of an aromatic ring current. Furthermore, the methyl groups gave a singlet at 2.96 ppm, a value that is nearly 0.4 ppm further downfield than the corresponding peak for free base **14**. More importantly, the internal protons showed pronounced upfield shifts. The NH protons afforded broad peaks at 7.31 ppm (2H) and 4.59 ppm (1H). The CH gave rise to a broadened resonance between 2.9 and 3.3 ppm, depending on the amount of TFA present in solution. These shifts are substantially larger than the values observed for the dications derived from benziporphyrin **5** and naphthiporphyrin **6**, which showed the inner CH resonances at 5.24 and 4.44 ppm, respectively. Hence, the presence of a pyrene unit within the porphyrinoid system appears to facilitate aromatic character to a substantially greater extent than benzene or naphthalene subunits. The carbon-13 NMR spectrum showed that the dication retained a plane of symmetry and the *meso*-carbons gave peaks at 93.9 and 120.6 ppm while the internal CH resonated at 102.6 ppm.

DOI: 10.1021/acs.joc.7b00829
J. Org. Chem. 2017, 82, 6680−6688

In order to further assess the aromatic characteristics of pyreniporphyrins, unsubstituted pyreniporphyrin **8** was assessed using density functional theory calculations at the DFT-B3LYP/6-311++G(d,p) level of theory. The calculated bond lengths for **8** (Figure 4) were consistent with a

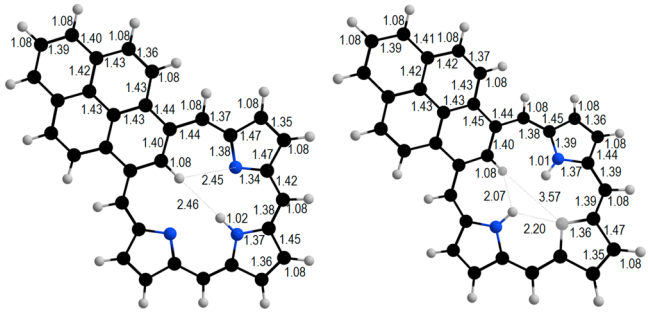

Figure 4. Calculated bond lengths (Å) for minimized pyreniporphyrin **8** (left) and the related dication $\mathbf{8H_2}^{2+}$ (right).

nonaromatic porphyrinoid showing significant bond length alternation within the macrocyclic framework. Furthermore, the pyrene subunit appears to be isolated from the conjugation pathway for the remaining structure. Dication $\mathbf{14H_2}^{2+}$ also shows some bond length alternation, but this is significantly reduced compared to the free base form. The free base can potentially exist in a number of tautomeric forms such as **8a**–**f**, none of which have global aromatic characteristics (Table 1). In addition to using B3LYP to calculate the relative energies, SPE calculations were performed on the minimized structures using M06-2*X*/6-311++G(d,p) and B3LYP-D3/6-311++G(d,p).[36,37] The relative energies obtained using these techniques were in good agreement, as had been noted previously in calculations for other carbaporphyrinoid structures.[13,38] Relative Gibbs free energies (ΔG) were also calculated, and these values were very similar indicating that entropic factors were not a significant contributor to the relative energies of these structures. As expected, tautomer **8a** proved to be the most stable due in part to the NH lying between two imine-type nitrogens as this optimizes hydrogen-bonding interactions. ΔE for tautomer **8b** was calculated to be 7.02−7.51 kcal/mol higher in energy due to the less optimal placement of the NH within the cavity. Interruption of the conjugation with bridging methylene bridges in tautomers **8c** and **8d** raised ΔE by 30.53−38.84 kcal/mol, even though this has no impact on the aromaticity of the system. However, disruption of the pyrene moiety by introducing CH_2 units at positions 2^2 or 2^3 in tautomers **8e** and **8f** leads to a massive increase in the relative energy of 61.38−64.48 kcal/mol relative to tautomer **8a**. Not only can this be attributed to the disruption of aromaticity in the pyrene subunit, but the introduction of a 16π electron antiaromatic pathway within the porphyrinoid core would also lead to destabilization.

Table 1. Calculated Relative Energies (kcal/mol) and NICS Values (ppm) for Pyreniporphyrin Tautomers[a]

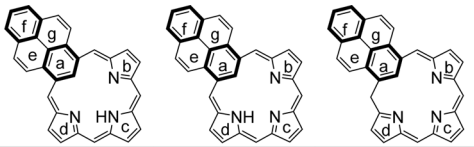

Molecule	**8a**	**8b**	**8c**
Rel. ΔG (298K)	0.00	+8.61	+38.42
B3LYP/B3LYP-D3	0.00/0.00	+7.02/+7.24	+38.27/+38.84
M06-2X	**0.00**	**+7.51**	**+35.40**
NICS(0)/NICS(1)$_{zz}$	+0.14/+2.46	+0.08/+2.22	+0.72/+5.13
NICS(a)/NICS(1a)$_{zz}$	**-4.92/-16.84**	**-5.76/-17.74**	**-7.01/-24.50**
NICS(b)/NICS(1b)$_{zz}$	-0.97/-7.40	-0.59/-6.80	-1.05/-8.40
NICS(c)/NICS(1c)$_{zz}$	-2.96/-13.40	-0.03/-6.60	+0.19/-5.83
NICS(d)/NICS(1d)$_{zz}$	-0.97/-7.40	-4.05/-8.88	+1.80/-2.63
NICS(e)/NICS(1e)$_{zz}$	-2.96/-13.40	-3.32/-14.54	-3.70/-15.07
NICS(f)/NICS(1f)$_{zz}$	**-9.96/-30.91**	**-10.02/-31.54**	**-10.70/-31.63**
NICS(g)/NICS(1g)$_{zz}$	-2.96/-13.40	-2.83/-12.67	-3.77/-14.01

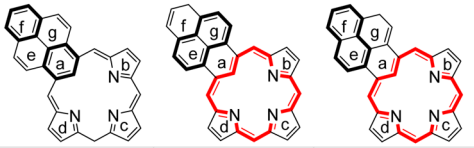

Molecule	**8d**	**8e**	**8f**
Rel. ΔG (298K)	+35.48	+63.13	+63.54
B3LYP/B3LYP-D3	+35.14/+35.42	+63.76/+64.38	+63.88/+64.48
M06-2X	**+30.53**	**+62.05**	**+61.38**
NICS(0)/NICS(1)$_{zz}$	+2.22/+9.81	**+19.12/+53.55**	**+16.30/+46.11**
NICS(a)/NICS(1a)$_{zz}$	**-7.96/-22.34**	-2.85/-5.84	-3.21/
NICS(b)/NICS(1b)$_{zz}$	-1.30/-7.31	**-2.27/-22.48**	**-2.31/-22.70**
NICS(c)/NICS(1c)$_{zz}$	+1.25/+6.40	-3.08/-6.20	-2.72/-6.61
NICS(d)/NICS(1d)$_{zz}$	**-0.17/-21.67**	-1.82/-10.54	-1.44/-10.58
NICS(e)/NICS(1e)$_{zz}$	-4.12/-14.16	**-7.74/-21.89**	**-7.33/-20.92**
NICS(f)/NICS(1f)$_{zz}$	**-10.63/-33.31**	+5.64/+8.73	**-9.23/-28.99**
NICS(g)/NICS(1g)$_{zz}$	-3.94/-16.90	**-8.54/-26.74**	+5.31/+8.67

[a]The presence of a paratropic ring current is highlighted in red.

The aromatic character of these molecules was assessed using the GIAO method, which has been consistently used as a reliable probe of porphyrinoid diatropic currents,[38−40] specifically using nucleus-independent chemical shifts (NICS).[41] In addition, the CSGT method with the ACID package was deployed to obtain ACID plots.[42] NICS considers the influence of σ and π electrons and is a less reliable measure of aromaticity. NICS$_{zz}$ calculations were performed 1 Å above the ring (NICS(1)$_{zz}$) and primarily show the effects due to the π-system.[43−46] It is worth noting that the shifts calculated using NICS(1)$_{zz}$ are much larger than those from regular NICS. The internal values for an aromatic system are usually <−5 ppm for NICS but may be <−20 ppm using NICS(1)$_{zz}$. While NICS(1)$_{zz}$ is considered to be more rigorous and the calculated results are shown in Table 1, both methods showed the same trends, and for this reason, only the NICS results will be discussed below. The NICS(0) values for macrocycles **8a** and **8b** were close to 0 as expected for a nonaromatic structure. The ACID plot for **8a** (Figure 5) also shows no indication of an aromatic conjugation pathway. The individual rings of the pyrene unit gave significantly negative values, particularly in the case of ring *f*. Pyrrole ring *c* in **8a** and pyrrole ring *d* in ring **8b** afforded moderately negative values consistent with some aromatic characteristics for these individual units, but the remaining pyrrolenine units showed negligible shifts. In

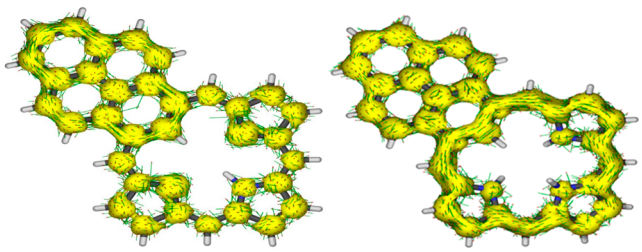

Figure 5. ACID plots (isovalue 0.07) of free base pyreniporphyrin **8a** and the related dication $\mathbf{8H_2}^{2+}$ demonstrating that only the protonated species possesses a macrocyclic ring current.

DOI: 10.1021/acs.joc.7b00829
J. Org. Chem. 2017, 82, 6680−6688

tautomers **8c** and **8d** all three pyrrolenine rings are nonaromatic, and the macrocycle also showed no indication of overall diatropicity. Tautomers **8e** and **8f** were more interesting as the core contains a 16π electron delocalization pathway. NICS(0) values for these structures were +19.12 and +16.30 ppm, respectively, in line with the expectation that strong paratropic ring currents would be present.

Calculations were also performed on mono- and diprotonated pyreniporphyrins (Table 2). Two monocations were considered, and **8a**H^+ was found to be between 2.57 and 2.86 kcal/mol more stable than **8b**H^+ due to more favorable hydrogen-bonding interactions in the former species. Both of these monocations showed significant global aromatic properties giving NICS(0) values of −5.84 and −5.09 ppm, respectively. In both cases, the protonated pyrrole units gave strongly negative results but the remaining pyrrolenine moieties gave low, essentially nonaromatic, values. The data indicate that these species favor 18-atom 18π electron aromatic conjugation pathways as illustrated in Figure 6. Dication **8**H_2^{2+} shows a further enhancement in aromatic character with a calculated NICS value of −8.93 ppm. In this case, all three pyrrole rings and ring *f* of the pyrene unit showed strongly negative values, while ring *a* gave a value of +3.55 ppm and rings *e* and *g* afforded moderate negative values. The aromatic properties of dication **8**H_2^{2+} and the substituted version **14**H_2^{2+} might be attributed to resonance contributors such as **14′**H_2^{2+} that possess 18π electron delocalization pathways. However, the NICS data are more consistent with a hybrid structure such as **14″**H_2^{2+} with a 19-atom 18π electron aromatic pathway. This interpretation is further supported by the ACID plot shown in Figure 5.

Table 2. Calculated Relative Energies (kcal/mol) and NICS Values (ppm) for Protonated Pyreniporphyrins

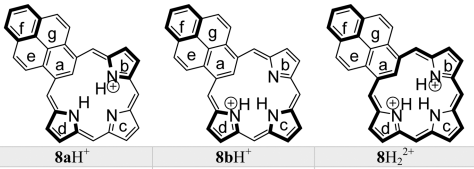

Molecule	**8a**H^+	**8b**H^+	**8**H_2^{2+}
Rel. DG (298K)	0.00	+3.10	*****
B3LYP/ B3LYP-D3	0.00/0.00	+2.86/+2.84	*****
M06-2X	**0.00**	**+2.57**	
NICS(0)/NICS(1)$_{zz}$	-5.84/-13.39	-5.09/-11.03	**-8.93/-19.83**
NICS(a)/NICS(1a)$_{zz}$	-2.61/-7.12	-1.10/-4.44	+3.55/+5.99
NICS(b)/NICS(1b)$_{zz}$	**-7.47/-16.50**	-1.72/-9.46	**-10.77/-19.23**
NICS(c)/NICS(1c)$_{zz}$	+0.34/-8.18	**-7.24/-22.10**	**-10.01/-36.66**
NICS(d)/NICS(1d)$_{zz}$	**-7.47/-16.50**	**-8.08/-15.36**	**-10.77/-19.23**
NICS(e)/NICS(1e)$_{zz}$	-3.17/-13.12	-3.04/-12.89	-2.76/-12.19
NICS(f)/NICS(1f)$_{zz}$	**-9.49/-31.72**	**-9.06/-30.46**	**-8.93/-25.02**
NICS(g)/NICS(1g)$_{zz}$	-3.17/-13.12	-2.87/-12.54	-2.76/-12.19

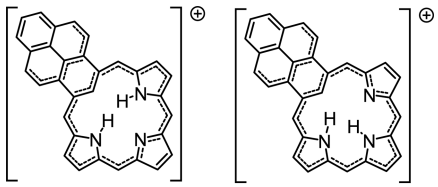

8aH^+ **8b**H^+

Figure 6. Proposed delocalization pathways in pyreniporphyrin monocations.

The feasibility of forming organometallic derivatives of pyreniporphyrin was investigated by reacting **14** with palladium(II) acetate in refluxing acetonitrile (Scheme 3). This resulted in the formation of palladium(II) complex **15** as a dark green powder in 91% yield. The UV−vis spectrum for **15** in dichloromethane showed three moderately strong absorptions at 350, 455, and 620 nm (Figure 7). For the proton NMR spectrum of **15** in $CDCl_3$, the *meso*-protons appeared as two 2H singlets at 7.26 and 8.72 ppm, values that are significantly downfield compared to the free base form of **14**. A 6H singlet for the methyl groups appeared at 2.70 ppm, again slightly downfield compared to the corresponding resonance for **14**. These data suggest that the metalated derivative possesses a weak diamagnetic ring current. The carbon-13 NMR spectrum confirmed the presence of a plane of symmetry and showed the *meso*-carbons at 95.6 and 118.5 ppm. The identity of **15** was also supported by high-resolution ESI mass spectrometry.

Scheme 3

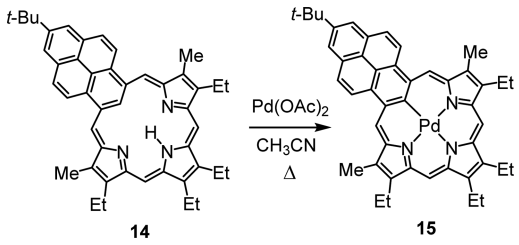

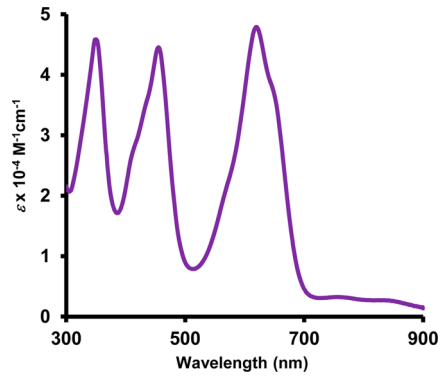

Figure 7. UV−vis spectrum of palladium(II) pyreniporphyrin in dichloromethane.

In order to access *meso*-tetraphenylpyreniporphyrins, the formation of pyrenitripyrrane **16** was investigated (Scheme 4). Reaction of dialdehyde **10** with excess phenylmagnesium bromide gave dicarbinol **17** as a mixture of diastereomers. Subsequent boron trifluoride etherate catalyzed condensation[30,31] of **17** with excess pyrrole in refluxing 1,2-dichloroethane yielded the required tripyrrane analogue **16** in 80% yield. However, attempts to react **16** with pyrrole and benzaldehyde in the presence of boron trifluoride etherate, followed by oxidation with DDQ, failed to give tetraphenylpyreniporphyrin **18**. Fortunately, condensation of **16** with thiophene dicarbinol **19** under similar conditions gave heteroanalogue **20**. Initially, when the reaction was carried out in dichloromethane, very low yields were obtained. However, switching the solvent to chloroform raised the yield to 7%. This solvent effect had previously been noted in the synthesis of sterically crowded *meso*-tetraarylporphyrinoids and was attributed to the activity of the Lewis acid catalyst being modified by the presence of ethanol (ethanol is generally used

DOI: 10.1021/acs.joc.7b00829
J. Org. Chem. 2017, 82, 6680−6688

Scheme 4

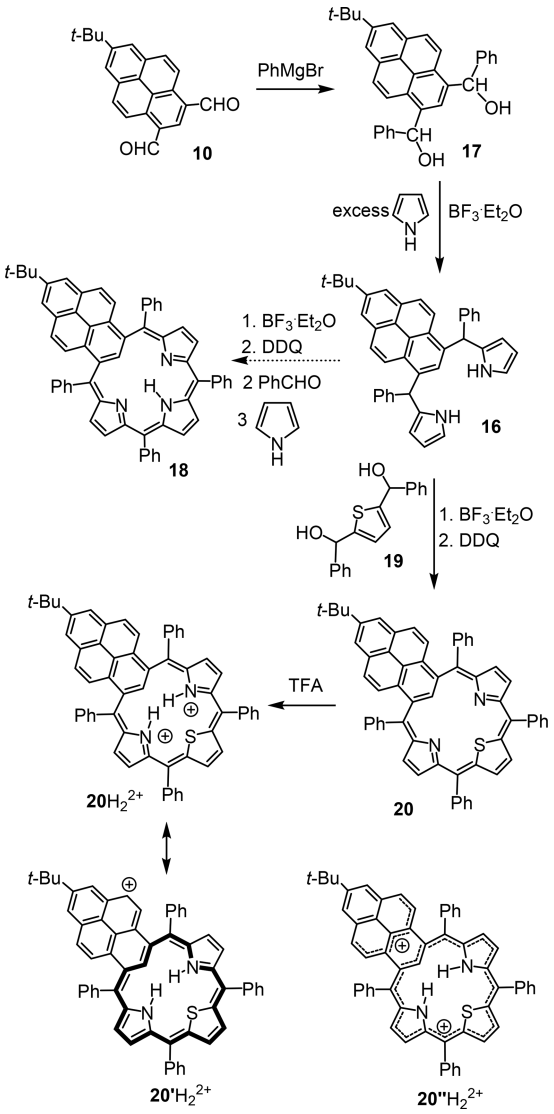

as a stabilizer in commercial grades of chloroform).[47−49] Further improvements in yield were obtained when 2% ethanol in dichloromethane was used as the reaction solvent, and these conditions raised the yield of **20** to >30%. The UV−vis spectrum for thiapyreniporphyrin **20** gave broad absorptions at 350, 379, and 636 nm (Figure 8). Addition of TFA gave a

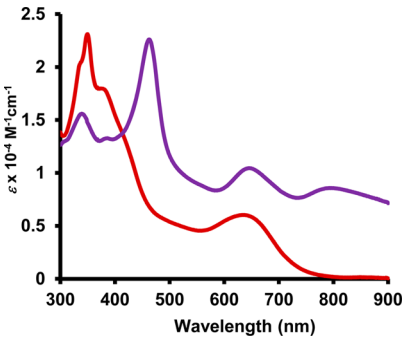

Figure 8. UV−vis spectra of thiapyreniporphyrin **20** in dichloromethane (free base, red line) and with 10 equiv of TFA in dichloromethane (dication $\mathbf{20}H_2^{2+}$, purple line).

diprotonated species $\mathbf{20}H_2^{2+}$, again showing relatively broad absorptions. The intermediacy of a monoprotonated cation $\mathbf{20}H^+$ was not easily discernible for this compound. The proton NMR spectrum demonstrated that **20** was nonaromatic and the external pyrrolic protons appeared at 6.66 (2H, d), 6.99 (2H, s) and 7.67 (2H, d), while the internal CH appeared at 7.58 ppm. The carbon-13 NMR spectrum was consistent with a symmetrical structure and showed the inner CH at 117.9 ppm. The proton NMR spectrum for the related dication $\mathbf{20}H_2^{2+}$ in TFA−$CDCl_3$ showed that the macrocycle was weakly diatropic. The pyrrolic protons shifted downfield to give peaks at 7.24 (2H, d), 7.99 (2H, s), and 8.22 ppm (2H, d), while the internal CH resonance shifted upfield to 5.33 ppm. The carbon-13 NMR spectrum was again consistent with a symmetrical structure and showed the inner CH resonance at 100.2 ppm.

Calculated bond lengths for unsubstituted thiapyreniporphyrin **9** showed the expected bond length alternation for a nonaromatic system, but this was somewhat reduced in the related dication $\mathbf{9}H_2^{2+}$ (Figure 9). NICS and $NICS_{zz}$

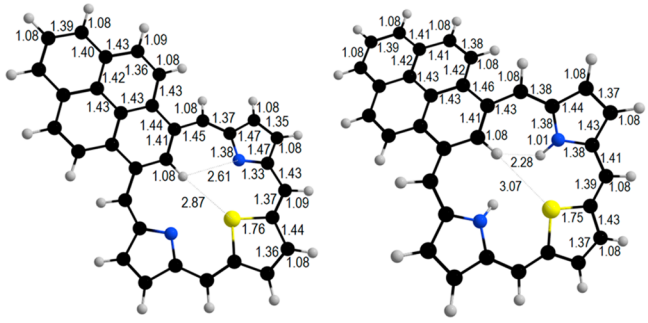

Figure 9. Bond lengths (Å) for minimized 24-thiapyreniporphyrin **9** (left) and the related dication $\mathbf{9}H_2^{2+}$ (right).

calculations were used to assess the aromatic characteristics of unsubstituted 24-thiapyreniporphyrin **9** and the related mono- and dications (Table 3). NICS(0) for **9** was very small

Table 3. Calculated NICS Values (ppm) for 24-Thiapyreniporphyrin and the Related Mono- and Dications

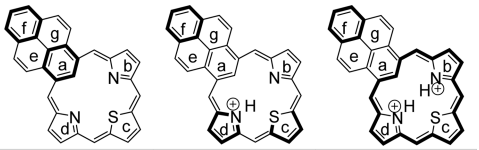

Molecule	**9**	$\mathbf{9}H^+$	$\mathbf{9}H_2^{2+}$
NICS(0)/$NICS(1)_{zz}$	-0.49/+2.17	-5.33/-11.05	**-9.36/-21.74**
NICS(a)/$NICS(1a)_{zz}$	**-5.82/-19.71**	-1.19/-4.72	+3.81/+10.15
NICS(b)/$NICS(1b)_{zz}$	-0.97/-8.74	-0.79/-9.99	**-10.58/-34.52**
NICS(c)/$NICS(1c)_{zz}$	-3.43/-4.58	**-8.48/-14.18**	**-13.17/-19.40**
NICS(d)/$NICS(1d)_{zz}$	-0.97/-8.74	**-8.22/-25.80**	**-10.58/-34.52**
NICS(e)/$NICS(1e)_{zz}$	-3.29/-12.86	-3.14/-12.46	-2.73/-10.72
NICS(f)/$NICS(1f)_{zz}$	**-10.23/-28.80**	**-9.00/-25.88**	**-6.42/-20.06**
NICS(g)/$NICS(1g)_{zz}$	-3.29/-12.86	-2.87/-11.29	-2.73/-10.72

and consistent with a nonaromatic species. The pyrene ring, particularly rings *a* and *g*, produced aromatic values, and thiophene ring *c* gave a moderately negative NICS value. However, pyrrolenine rings *b* and *d* appeared to be nonaromatic. Monoprotonation to give $\mathbf{9}H^+$ resulted in an aromatic NICS(0) value of −5.33 ppm, while the diprotonated species $\mathbf{9}H_2^{2+}$ gave a strongly aromatic value of −9.36 ppm. In $\mathbf{9}H^+$, rings *c*, *d*, and *f* showed strongly aromatic values while ring *b*

DOI: 10.1021/acs.joc.7b00829
J. Org. Chem. 2017, 82, 6680−6688

appeared to be nonaromatic. This result suggests that a similar conjugation pathway to the one shown for **8b**H$^+$ in Figure 6 is favored in this case. Dication **9**H$_2^{2+}$ afforded large negative values for rings *b*, *c*, *d*, and *f*, and this result indicates that hydrid structures like **20**″H$_2^{2+}$ are favored over resonance forms such as **20**′H$_2^{2+}$ (Scheme 4). The ACID plot for **9**H$_2^{2+}$ is also consistent with the presence of a 19-atom 18π electron delocalization pathway (Figure 10). In fact, the proton NMR

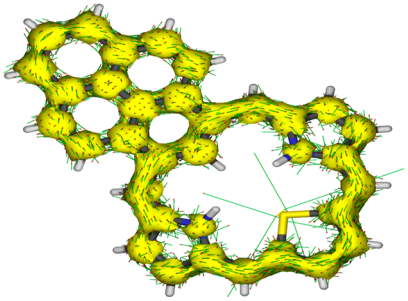

Figure 10. AICD plot (isovalue 0.07) of thiapyreniporphyrin dication **9**H$_2^{2+}$ showing the presence of a diatropic ring current.

data shows that **20**H$_2^{2+}$ is far less aromatic than predicted by the NICS or ACID results. This undoubtedly results from the *meso*-phenyl substituents causing severe distortions to the macrocycle due to steric congestion.

CONCLUSIONS

PAH−porphyrin hybrids with a pyrene unit in place of a pyrrole moiety have been prepared using two different "3 + 1" strategies. Condensation of a pyrene dialdehyde with a tripyrrane gave a nonaromatic pyreniporphyrin that showed striking diatropic characteristics upon protonation. Reaction with palladium(II) acetate afforded a stable organometallic derivative that showed weak diatropicity. A tripyrrane analogue was prepared by reacting a pyrene dicarbinol with excess pyrrole and this intermediate was used to synthesize a thiapyreniporphyrin. This macrocycle was also nonaromatic in the free base form but took on some global aromatic character upon protonation. NICS calculations and ACID plots were used to gain a better understanding of the aromatic characteristics of pyreniporphyrins. These results demonstrate that large polycyclic aromatic hydrocarbon units can be introduced into the porphyrin framework, and it may be possible to further extend this work to form graphene-like PAH−porphyrin hybrids.

EXPERIMENTAL SECTION

Melting points are uncorrected. NMR spectra were recorded using a 400 or 500 MHz NMR spectrometer and were run at 300 K unless otherwise indicated. ^{1}H NMR values are reported as chemical shifts δ, relative integral, multiplicity (s, singlet; d, doublet; t, triplet; q, quartet; m, multiplet; br, broad peak) and coupling constant (*J*). Chemical shifts are reported in parts per million (ppm) relative to $CDCl_3$ (^{1}H residual $CHCl_3$ δ 7.26, ^{13}C $CDCl_3$ triplet δ 77.23) or d_6-DMSO (residual d_5-DMSO ^{1}H resonance δ 2.49 ppm, ^{13}C septet δ 39.7 ppm), and coupling constants were taken directly from the spectra. NMR assignments were made with the aid of ^{1}H−^{1}H COSY, HSQC, DEPT-135, and NOE difference proton NMR spectroscopy. 2D experiments were performed using standard software. High-resolution mass spectra (HRMS) were carried out using a double focusing magnetic sector instrument. ^{1}H and ^{13}C NMR spectra for all new compounds are provided in the Supporting Information.

2-*tert*-Butyl-6,8-diformylpyrene (10). A mixture of tribromopyrene **12**[34] (5.56 g, 11.3 mmol) in THF (120 mL) was cooled to −70 °C with the aid of a dry ice−acetone bath. *n*-Butyllithium (2.56 M in hexane, 100 mL, 164 mmol) was added and the resulting mixture stirred at −70 °C for 3 h. DMF (20 mL, 259 mmol) was added in one portion, and the resulting solution was stirred for 40 min under the same conditions. A saturated ammonium chloride solution (30 mL) was added to quench the reaction. After filtration, the aqueous layer was extracted three times with dichloromethane, and the combined organic layers were washed sequentially with saturated sodium bicarbonate solution and saturated sodium chloride solution. The organic solution was dried over sodium sulfate, filtered, and evaporated under reduced pressure, and the residue purified by column chromatography on alumina eluting with toluene. Evaporation of the product fractions gave the diformylpyrene (2.56 g, 8.15 mol, 73%) as a yellow powder. Mp: 264−268 °C (lit. mp[34] 267 °C). ^{1}H NMR (500 MHz, $CDCl_3$): δ 1.63 (9H, s, *t*-Bu), 8.496 (2H, s, 6,8-H), 8.500 (2H, d, *J* = 9.2 Hz, 5,9-H), 8.87 (1H, s, 2-H), 9.53 (2H, d, *J* = 9.2 Hz, 4,10-H), 10.82 (2H, s, 2 × CHO). ^{13}C NMR (125 Hz, $CDCl_3$): δ 32.0, 35.6, 121.9, 123.1, 125.0, 126.5, 126.8, 130.4, 134.3, 134.4, 137.4, 151.0, 192.4.

8,19-Dimethyl-9,13,14,18-tetraethyl-2^4-*tert*-butylpyreniporphyrin (14). In a pear-shaped flask, freshly prepared tripyrrane dicarboxylic acid **13** (50.0 mg, 0.110 mmol) was stirred with trifluoroacetic acid (1.0 mL) under nitrogen for 2 min. Dichloromethane (30 mL) was added, followed immediately by dialdehyde **10** (35.0 mg, 0.111 mmol), and the mixture was stirred under nitrogen at room temperature for a further 5 h. DDQ (27.0 mg, 0.119 mmol) was added and the resulting solution was stirred under the same conditions for 3 h. The mixture was washed with water and chromatographed twice on grade 3 alumina, eluting with a 7:3 mixture of dichloromethane and hexanes. A dark green fraction was collected and recrystallized from chloroform−methanol to give the pyreniporphyrin (27 mg, 0.042 mmol, 38%) as a dark green powder. Mp: >300 °C. UV−vis (1% Et_3N−CH_2Cl_2): λ_{max} (log ε) 343 (4.61), 446 (4.62), 464 (sh, 4.58), 553 (sh, 4.15), 590 (4.24), 632 nm (4.09). UV−vis (1 equiv TFA−CH_2Cl_2): λ_{max} (log ε) 339 (4.62), 396 (sh, 4.39), 443 (4.51), 469 (sh, 4.41), 496 (sh, 4.31), 621 (4.11), 677 (4.80), 803 nm (3.84). UV−vis (1% TFA−CH_2Cl_2): λ_{max} (log ε) 363 (4.58), 412 (4.45), 462 (4.55), 486 (sh, 4.50), 727 (4.67), 770 nm (sh, 4.48). ^{1}H NMR (500 MHz, $CDCl_3$): δ 1.29 (6H, t, *J* = 7.6 Hz, 9,18-CH_2CH_3), 1.35 (6H, t, *J* = 7.6 Hz, 13,14-CH_2CH_3), 1.62 (9H, s, *t*-Bu), 2.59 (6H, s, 8,19-CH_3), 2.78 (4H, q, *J* = 7.6 Hz, 9,18-CH_2), 2.82 (4H, q, *J* = 7.6 Hz, 13,14-CH_2), 6.49 (2H, s, 11,16-H), 8.27 (2H, d, *J* = 9.3 Hz, 2^2,4^2-H), 8.31 (2H, s, 2^3,4^3-H), 8.36 (2H, s, 6,21-H), 8.47 (1H, s, 22-H), 8.98 (2H, d, *J* = 9.3 Hz), 2^1,4^1-H), 9.88 (1H, br s, NH). ^{13}C NMR (125 MHz, $CDCl_3$): δ 10.9 (8,19-CH_3), 15.5 (9,18-CH_2CH_3), 16.1 (13,14-CH_2CH_3), 18.1 (13,14-CH_2), 18.6 (9,18-CH_2), 32.1 ($C(CH_3)_3$), 35.4 ($C(CH_3)_3$), 93.3 (11.16-CH), 116.5 (6,21-CH), 119.3 (22-CH), 123.9 (2^1,4^1-CH), 124.7 (2^3,4^3-CH), 126.7, 127.7, 130.2 (2^2,4^2-CH), 131.2, 134.2, 140.3, 140.9, 141.8, 148.1, 149.7, 157.1, 169.9. ^{1}H NMR (500 MHz, TFA−$CDCl_3$, dication **14**H$_2^{2+}$): δ 1.41 (6H, t, *J* = 7.7 Hz), 1.45 (6H, t, *J* = 7.7 Hz) (4 × CH_2CH_3), 1.64 (9H, s, *t*-Bu), 2.90 (1H, s, 22-CH), 2.96 (6H, s, 8,19-CH_3), 3.14−3.19 (8H, 2 overlapping quartets, 4 × CH_2CH_3), 4.59 (1H, br s, 24-NH), 7.31 (2H, br s, 23,25-NH), 7.65 (2H, s, 11,16-H), 8.61 (2H, s, 2^3,4^3-H), 8.67 (2H, d, *J* = 9.0 Hz, 2^2,4^2-H), 8.93 (2H, d, *J* = 9.0 Hz, 2^1,4^1-H), 9.37 (2H, s, 6,21-H). ^{13}C NMR (125 MHz, TFA−$CDCl_3$, dication **14**H$_2^{2+}$): δ 11.2 (8,19-CH3), 14.8, 15.7 (4 × CH_2CH_3), 18.6, 18.8 (4 × CH_2CH_3), 32.8 ($C(CH_3)_3$), 35.7 ($C(CH_3)_3$), 93.9 (11.16-CH), 102.6 (22-CH), 120.6 (6,21-CH), 122.7, 126.0, 126.6 (2^1,4^1-CH), 127.5, 131.01 ((2^1,4^1-CH), 131.1, 136.7 (2^2,4^2-CH), 139.2, 141.1, 142.6, 145.8, 146.5, 150.7, 152.6, 158.2. HRMS (ESI): calcd for $C_{46}H_{47}N_3$ + H 642.3848, found 642.3840.

[8,19-Dimethyl-9,13,14,18-tetraethyl-2^4-*tert*-butylpyreniporphyrinato]palladium(II) (15). Pyreniporphyrin **14** (8.0 mg, 0.0125 mmol) and palladium(II) acetate (6.0 mg, 0.027 mmol) in a 1:1 mixture of chloroform and acetonitrile (20 mL) were stirred under reflux for 2 h. The solution was allowed to cool to room temperature, washed with water, and extracted with dichloromethane. The

DOI: 10.1021/acs.joc.7b00829
J. Org. Chem. 2017, 82, 6680−6688

combined organic layers were evaporated under reduced pressure. The residue was purified by column chromatography on grade 3 basic alumina, eluting with a 4:1 mixture of dichloromethane and hexanes, and a bluish-green fraction was collected. The solvent was evaporated under reduced pressure and the residue recrystallized from chloroform−methanol to afford the palladium complex (8.5 mg, 0.0114 mmol, 91%) as a dark green powder. Mp: >300 °C. UV−vis (1% $Et_3N-CH_2Cl_2$): λ_{max} (log ε): 350 (4.66), 455 (4.65), 620 (4.68), 759 (3.51), 837 nm (3.43). ^{1}H NMR (500 MHz, $CDCl_3$): δ 1.39 (6H, t, J = 7.6 Hz), 1.44 (6H, t, J = 7.6 Hz) (4 × CH_2CH_3), 1.62 (9H, s, t-Bu), 2.70 (6H, s, 8,19-CH_3), 2.96−3.02 (8H, m, 4 × CH_2CH_3), 7.26 (2H, s, 11,16-CH), 8.21 (2H, d, 2^2,4^2-CH, J = 9.3 Hz), 8.27 (2H, s, 2^3,4^3-CH), 8.72 (2H, s, 6,21-CH), 8.97 (2H, d, J = 9.3 Hz, 2^1,4^1-CH). ^{13}C NMR (125 Hz, $CDCl_3$): δ 10.4 (8,19-CH_3), 15.2, 16.5 (4 × CH_2CH_3), 18.4, 18.6 (4 × CH_2CH_3), 31.8 ($C(CH_3)_3$), 35.2 ($C(CH_3)_3$), 95.6 (11,16-CH), 118.5 (6,21-CH), 122.9, 125.1 (21,41-CH), 125.2 (2^3,4^3-CH), 127.3, 129.6 (2^2,4^2-CH), 130.6, 138.1, 139.8, 140.5, 143.3, 144.4, 149.4, 152.2. HRMS (ESI) calcd for $C_{46}H_{45}N_3Pd$ + H: 746.2727. Found: 446.2726.

1,3-Bis(phenylhydroxymethyl)-7-*tert*-butylpyrene (17). Dialdehyde **10** (0.50 g, 1.6 mmol) was dissolved in THF (75 mL). and the solution was cooled to 0 °C. Phenylmagnesium bromide (1 M in THF, 5 mL) was added dropwise via syringe. The resulting mixture was stirred at 0 °C for 3 h. Saturated ammonium chloride was added to quench the reaction mixture. The organic layer was diluted with diethyl ether, washed three times with water, and dried over sodium sulfate, and the solvent was evaporated under reduced pressure. The resulting solid was recrystallized from chloroform−hexane to yield the dicarbinol (0.395 g, 0.84 mmol, 52%) as a pale-yellow powder that consisted of a mixture of diastereomers. Mp: 231−233 °C. ^{1}H NMR (500 MHz, d_6-DMSO): δ 1.50 (9H, s, t-Bu), 6.23 (d, J = 4.2 Hz), 6.27 (d, J = 4.2 Hz) (2H, 2 × OH), 6.71 (d, J = 4.2 Hz), 6.74 (d, J = 4.2 Hz) (2H, 2 × CHOH), 7.15−7.19 (2H, m,2 × p-H), 7.24−7.29 (4H, m, 4 × m-H), 7.41−7.45 (4H, m, 4 × o-H), 8.05−8.08 (2H, two overlapping doublets, J = 9.3 Hz), 8.250 (s), 8.254 (s) (2H, 6,8-H), 8.41 (d, J = 9.3 Hz), 8.43 (d, J = 9.3 Hz) (2H), 8.55 (s), 8.62 (s) (1H, 2-H). ^{13}C NMR (125 MHz, d_6-DMSO): δ 31.8, 35.1, 71.7, 72.1, 122.3, 122.7, 123.58, 123.63, 123.8, 124.1, 124.5, 124.7, 126.3, 126.4, 126.80, 126.85, 127.0, 127.09, 127.13, 128.14, 128.18, 130.4, 138.4, 138.5, 145.50, 145.54, 148.8. HRMS (ESI): calcd for $C_{34}H_{30}O_2$ 470.2246, found 470.2240.

1,3-Bis(phenyl-2-pyrrolylmethyl)-7-*tert*-butylpyrene (16). Nitrogen was bubbled through a solution of dicarbinol **17** (150.0 mg, 0.319 mmol) and pyrrole (4 mL) in 1,2-dichloroethane (20 mL) for 20 min, after which 60 μL of a 10% boron trifluoride etherate solution in dichloromethane was added, and the resulting mixture was stirred under reflux for 24 h. The solution was cooled to room temperature and quenched by addition of triethylamine (2 mL). The solvent was evaporated on a rotary evaporator initially using a water aspirator, and excess pyrrole was removed with the aid of a vacuum pump. The product was purified by column chromatography on silica, eluting with dichloromethane. Evaporation of the product fractions gave the pyrenitripyrrane (145 mg, 0.255 mmol, 80%) as a pale-yellow oil that solidified upon standing. As expected, the product consisted on a mixture of diastereomers. ^{1}H NMR (500 MHz, $CDCl_3$): δ 1.60 (9H, s, t-Bu), 5.78−5.80 (m), 5.81−5.83 (m) (2H, 2 × pyrrole 3-H), 6.11−6.13 (m), 6.14−6.16 (m) (2H, 2 × pyrrole 4-H), 6.482 (s), 6.487 (s) (2H, 2 × bridge-CH), 6.59−6.61 (m), 6.62−6.64 (m) (2H, 2 × pyrrole 5-H), 7.11−7.17 (4H, m), 7.20−7.30 (6H, m) (2 × Ph), 7.34 (s), 7.36 (s) (1H, 2-H), 7.67 (br s), 7.70 (br s) (2H, 2 × NH), 8.03 (2H, d, J = 9.3 Hz, 5,9-H), 8.22 (2H, s, 6,8-H), 8.26−8.28 (2H, two overlapping doublets, 4,10-H). ^{13}C NMR (125 MHz, $CDCl_3$): δ 32.0, 35.3, 47.01, 47.05, 108.38, 108.45, 108..50, 117.34, 117.41, 122.8, 123.2, 123.4, 125.7, 126.72, 126.78, 127.9, 128.0, 128.35, 128.37, 128.6, 128.7, 129.1, 131.0, 133.4, 133.5, 136.43, 136.46, 143.3, 143.4, 149.3. HRMS (ESI): calcd for $C_{42}H_{36}N_2$ + H 569.2957, found 569.2947.

6,11,16,21-Tetraphenyl-2^4-*tert*-butyl-28-thiapyreniporphyrin (20). Nitrogen was bubbled through a solution of pyrenitripyrrane **16** (54 mg, 0.095 mmol) and thiophene dicarbinol **19** (30.0 mg, 0.101 mmol) in dichloromethane (30 mL) and ethanol (0.6 mL) for 10 min. A 10% solution of $BF_3{\cdot}Et_2O$ in dichloromethane (50 μL) was added by syringe, and the solution was allowed to stir under nitrogen in the dark at room temperature for 3 h. DDQ (65 mg, 0.286 mmol) was added, and stirring was continued for a further 5 h. The solvent was removed under reduced pressure, and the residue purified by column chromatography on grade 3 neutral alumina eluting with dichloromethane and then on grade 3 neutral alumina eluting with a 3:2 ratio of dichloromethane and hexanes. A dark green band was collected and the solvent evaporated under reduced pressure. The residue was recrystallized from chloroform−methanol to afford thiapyreniporphyrin **20** (25.5 mg, 0.0363 mmol, 31%) as a dark green powder. Mp: >300 °C. UV−vis (CH_2Cl_2): λ_{max} (log ε) 335 (sh, 6.61), 350 (4.67), 379 (sh, 4.55), 636 nm (4.08). UV−vis (1% TFA−CH_2Cl_2): λ_{max} (log ε) 339 (4.49), 463 (4.66), 644 (4.32), 796 nm (4.23). ^{1}H NMR (500 MHz, $CDCl_3$): δ 1.49 (9H, s, t-Bu), 6.66 (2H, d, J = 4.8 Hz, 9,18-CH), 6.99 (2H, s, 13,14-CH), 7.37−7.45 (16H, m), 7.58 (1H, s, 22-CH), 7.63−7.66 (4H, m, 6,21-o-Ph), 7.67 (2H, d, J = 4.8 Hz, 8,19-CH), 7.85 (2H, d, J = 9.2 Hz, 2^2,4^2-H), 7.96 (2H, d, J = 9.2 Hz, 2^1,4^1-H), 8.07 (2H, s, 2^3,4^3-CH). ^{13}C NMR (125 Hz, $CDCl_3$): δ 32.0 ($C(CH_3)_3$, 35.3 ($C(CH_3)_3$), 117.9 (22-CH), 123.0 (2^3,4^3-CH), 123.1, 126.3 (2^1,4^1-CH), 126.5, 127.9 (2^2,4^2-CH), 128.2, 128.4, 128.6, 129.26, 129.30, 130.0, 130.7, 131.1, 131.2 (9,18-CH), 131.9, 135.48, 135.51 (8,19-CH and 13,14-CH), 135.9, 138.8, 141.8, 146.4, 149.3, 155.1, 157.2, 171.1. ^{1}H NMR (500 MHz, TFA−$CDCl_3$, 50 °C, dication **20**H_2^{2+}): δ 1.51 (9H, s, t-Bu), 5.33 (1H, s, 22-H), 7.24 (2H, d, J = 5.1 Hz, 9,18-H), 7.61−7.71 (14H, m), 7.84−7.86 (4H, m, 2^1,4^1-H and 2 × o-Ph), 7.99 (2H, s, 13,14-H), 8.06 (2H, d, J = 9.3 Hz, 2^2,4^2-H), 8.22 (2H, d, J = 5.1 Hz, 8,19-H), 8.29 (2H, s, 2^3,4^3-CH). ^{13}C NMR (500 MHz, TFA-$CDCl_3$, dication **20**H_2^{2+}): δ 31.8, 35.6, 100.2 (22-CH), 121.8, 127.68, 127.76, 127.9, 128.8, 129.1, 129.79, 129.86, 130.2, 131.5, 132.5, 132.8, 133.5, 134.1, 134.5, 135.4, 139.2, 140.5, 141.3, 144.3, 152.4, 154.24, 154.31, 163.3. HRMS (ESI): calcd for $C_{60}H_{42}N_2S$ + H 823.3147, found 823.3133.

Computational Studies. All calculations were performed using the Gaussian 09[50] suite of programs running on a Linux-based PC. Energy minimization calculations were using B3LYP6-311++G(d,p). The resulting Cartesian coordinates can be found in the Supporting Information. Frequency calculations were performed at the same level of theory to confirm the nature of convergence. Single-point energy calculations with M06/6-311++G(d,p), and B#LYP-D3LYP-D3/6-311++G(d,p) were performed to probe the effects of dispersion on the relative energies. Two types of NMR calculations were performed: the GIAO method[51] was used to obtain NICS values and CGST to obtain ACID plots.[43] NICS(0) was calculated at the mean position of the four heavy atoms in the middle of the macrocycle. NICS(a), NICS(b), NICS(c), NICS(d), NICS(e), NICS(f), and NICS(g) values were obtained by applying the same method to the mean position of the heavy atoms that comprise the individual rings of each macrocycle. In addition, NICS(1)$_{zz}$, NICS(1a)$_{zz}$, NICS(1b)$_{zz}$, NICS(1c)$_{zz}$, NICS(1d)$_{zz}$, NICS(1e)$_{zz}$, NICS(1f)$_{zz}$, and NICS(1g)$_{zz}$ were obtained by applying the same method to ghost atoms placed 1 Å above each of the corresponding NICS(0) points and extracting the zz contribution of the magnetic tensor.[42,52] ACID plots for all the compounds were computed at two different isovalues, 0.05 (standard) and 0.07. These can also be found in the Supporting Information.

■ ASSOCIATED CONTENT

Supporting Information

The Supporting Information is available free of charge on the ACS Publications website at DOI: 10.1021/acs.joc.7b00829.

Tables giving Cartesian coordinates, calculated energies, and AICD plots for all of the calculated tautomers and selected ^{1}H NMR, ^{1}H−^{1}H COSY, HMQC, ^{13}C NMR, DEPT-135, MS, and UV−vis spectra (PDF)

DOI: 10.1021/acs.joc.7b00829
J. Org. Chem. 2017, 82, 6680−6688

AUTHOR INFORMATION

Corresponding Author

*E-mail: tdlash@ilstu.edu.

ORCID

Timothy D. Lash: 0000-0002-0050-0385

Notes

The authors declare no competing financial interest.

ACKNOWLEDGMENTS

This work was supported by the National Science Foundation under Grant Nos. CHE-1212691 and CHE-1465049 and the Petroleum Research Fund, administered by the American Chemical Society.

REFERENCES

(1) Lash, T. D. *Chem. Rev.* **2017**, *117*, 2313−2446.
(2) Lash, T. D.; Hayes, M. J. *Angew. Chem., Int. Ed. Engl.* **1997**, *36*, 840−842.
(3) Li, D.; Lash, T. D. *J. Org. Chem.* **2014**, *79*, 7112−7121.
(4) Lash, T. D. *Acc. Chem. Res.* **2016**, *49*, 471−482.
(5) Bergman, K. M.; Ferrence, G. M.; Lash, T. D. *J. Org. Chem.* **2004**, *69*, 7888−7897.
(6) (a) Srinivasan, A.; Furuta, H. Confusion Approach to Porphyrinoid Chemistry. *Acc. Chem. Res.* **2005**, *38*, 10−20. (b) . Toganoh, M.; Furuta, H. Synthesis and Metal Coordination of N-Confused and N-Fused Porphyrinoids. In *Handbook of Porphyrin Science − With Applications to Chemistry, Physics, Material Science, Engineering, Biology and Medicine*; Kadish, K. M., Smith, K. M., Guilard, R., Eds.; World Scientific Publishing: Singapore, 2010; Vol. 2, pp 103−192.
(7) Lash, T. D. *Org. Biomol. Chem.* **2015**, *13*, 7846−7878.
(8) Lash, T. D.; Muckey, M. A.; Hayes, M. J.; Liu, D.; Spence, J. D.; Ferrence, G. M. *J. Org. Chem.* **2003**, *68*, 8558−8570.
(9) Lash, T. D.; Colby, D. A.; El-Beck, J. A.; AbuSalim, D. I.; Ferrence, G. M. *Inorg. Chem.* **2015**, *54*, 9174−9187.
(10) Lash, T. D. *Chem. - Asian J.* **2014**, *9*, 682−705.
(11) Lash, T. D.; Chaney, S. T.; Richter, D. T. *J. Org. Chem.* **1998**, *63*, 9076−9088.
(12) Lash, T. D.; Yant, V. R. *Tetrahedron* **2009**, *65*, 9527−9535.
(13) AbuSalim, D. I.; Lash, T. D. *Org. Biomol. Chem.* **2014**, *12*, 8719−8736.
(14) Richter, D. T.; Lash, T. D. *Tetrahedron* **2001**, *57*, 3657−3671.
(15) Lash, T. D.; Szymanski, J. T.; Ferrence, G. M. *J. Org. Chem.* **2007**, *72*, 6481−6492.
(16) Lash, T. D. *Angew. Chem., Int. Ed. Engl.* **1995**, *34*, 2533−2535.
(17) Lash, T. D.; Young, A. M.; Rasmussen, J. M.; Ferrence, G. M. *J. Org. Chem.* **2011**, *76*, 5636−5651.
(18) Stepien, M.; Gonka, E.; Zyla, M.; Sprutta, N. *Chem. Rev.* **2017**, *117*, 3479−3716.
(19) (a) Kopranenkov, V. N.; Vorotnikov, A. M.; Luk'yanets, E. A. *J. Gen. Chem. USSR* **1979**, *49*, 2467. (b) Rein, M.; Hanack, M. *Chem. Ber.* **1988**, *121*, 1601−1608. (c) Ito, S.; Ochi, N.; Uno, H.; Murashima, T.; Ono, N. *Chem. Commun.* **2000**, 893−894. (d) Finikova, O. S.; Cheprakov, A. V.; Carroll, P. J.; Vinogradov, S. A. *J. Org. Chem.* **2003**, *68*, 7517−7520. (e) Finikova, O. S.; Aleshchenkov, S. E.; Briñas, R. P.; Cheprakov, A. V.; Carroll, P. J.; Vinogradov, S. A. *J. Org. Chem.* **2005**, *70*, 4617−4628. (f) Finikova, O. S.; Cheprakov, A. V.; Vinogradov, S. A. *J. Org. Chem.* **2005**, *70*, 9562−9572. (g) Manley, J. M.; Roper, T. J.; Lash, T. D. *J. Org. Chem.* **2005**, *70*, 874−891.
(20) Novak, B. H.; Lash, T. D. *J. Org. Chem.* **1998**, *63*, 3998−4010.
(21) Lash, T. D.; Chandrasekar, P.; Osuma, A. T.; Chaney, S. T.; Spence, J. D. *J. Org. Chem.* **1998**, *63*, 8455−8469.
(22) (a) Uno, H.; Cai, C.; Uoyama, H.; Nakamura, M. *Heterocycles* **2012**, *84*, 829−841. (b) Filatov, M. A.; Baluschev, S.; Ilieva, I. Z.; Enkelmann, V.; Miteva, T.; Landfester, K.; Aleshchenkov, S. E.; Cheprakov, A. V. *J. Org. Chem.* **2012**, *77*, 11119−11131.
(23) Lash, T. D.; Werner, T. M.; Thompson, M. L.; Manley, J. M. *J. Org. Chem.* **2001**, *66*, 3152−3159.
(24) Gandhi, V.; Thompson, M. L.; Lash, T. D. *Tetrahedron* **2010**, *66*, 1787−1799.
(25) Boedigheimer, H.; Ferrence, G. M.; Lash, T. D. *J. Org. Chem.* **2010**, *75*, 2518−2527.
(26) Ota, K.; Tanaka, T.; Osuka, A. *Org. Lett.* **2014**, *16*, 2974−2977.
(27) Gopee, H.; Kong, X.; He, Z.; Chambrier, D. L.; Hughes, D. L.; Tizzard, G. J.; Coles, S. J.; Cammidge, A. N. *J. Org. Chem.* **2013**, *78*, 9505−9511.
(28) Szyszko, B.; Bialonska, A.; Szterenberg, L.; Latos-Grazyński, L. *Angew. Chem., Int. Ed.* **2015**, *54*, 4932−4936.
(29) Szyszko, B.; Malecki, M.; Berlicka, A.; Bialek, M. J.; Bialonska, A.; Kupietz, K.; Pacholska-Dudziak, E.; Latos-Grazyński, L. *Chem. - Eur. J.* **2016**, *22*, 7602−7608.
(30) Lash, T. D.; Toney, A. M.; Castans, K. M.; Ferrence, G. M. *J. Org. Chem.* **2013**, *78*, 9143−9152.
(31) Fosu, S. C.; Ferrence, G. M.; Lash, T. D. *J. Org. Chem.* **2014**, *79*, 11061−11074.
(32) These results were presented, in part, at the 251st National Meeting of the American Chemical Society: Gao, R.; Lash, T. D. Abstracts of Papers. *251st National Meeting of the American Chemical Society*; San Diego, CA, Mar 2016; American Chemical Society: Washington, DC, 2016; ORGN-666.
(33) Lash, T. D. *J. Porphyrins Phthalocyanines* **2016**, *20*, 855−888.
(34) Inoue, J.; Fukui, K.; Kubo, T.; Nakazawa, S.; Sato, K.; Shiomi, D.; Morita, Y.; Yamamoto, K.; Takui, T.; Nakasuji, K. *J. Am. Chem. Soc.* **2001**, *123*, 12702−12703.
(35) Medforth, C. J. In *The Porphyrin Handbook*; Kadish, K. M., Smith, K. M., Guilard, R., Eds.; Academic Press: San Diego, 2000; Vol. 5, pp 1−80.
(36) Zhao, Y.; Truhlar, D. G. *Theor. Chem. Acc.* **2008**, *120*, 215−241.
(37) Grimme, S. *J. Comput. Chem.* **2004**, *25*, 1463−1473.
(38) (a) AbuSalim, D. I.; Lash, T. D. *J. Org. Chem.* **2013**, *78*, 11535−11548. (b) AbuSalim, D. I.; Lash, T. D. *Org. Biomol. Chem.* **2013**, *11*, 8306−8323. (c) AbuSalim, D. I.; Lash, T. D. *J. Phys. Chem. A* **2015**, *119*, 11440−11453.
(39) Toganoh, M.; Furuta, H. *J. Org. Chem.* **2013**, *78*, 9317−9327.
(40) AbuSalim, D. I.; Ferrence, G. M.; Lash, T. D. *J. Am. Chem. Soc.* **2014**, *136*, 6763−6772.
(41) Schleyer, P. v. R.; Maerker, C.; Dransfeld, A.; Jiao, H.; Hommes, N. J. R. v. E. *J. Am. Chem. Soc.* **1996**, *118*, 6317−6318.
(42) Geuenich, D.; Hess, K.; Kohler, F.; Herges, R. *Chem. Rev.* **2005**, *105*, 3758−3772.
(43) Corminboeuf, C.; Heine, T.; Seifert, G.; Schleyer, P. v. R.; Weber, J. *Phys. Chem. Chem. Phys.* **2004**, *6*, 273−276.
(44) Fallah-Bagher-Shaidaei, H.; Wannere, C. S.; Corminboeuf, C.; Puchta, R.; Schleyer, P. v. R. *Org. Lett.* **2006**, *8*, 863−866.
(45) Mills, N. S.; Llagostera, K. B. *J. Org. Chem.* **2007**, *72*, 9163−9169.
(46) Solà, M.; Feixas, F.; Jiménez-Halla, J. O. C.; Matito, E.; Poater, J. *Symmetry* **2010**, *2*, 1156−1179.
(47) Lindsey, J. S.; Wagner, R. W. *J. Org. Chem.* **1989**, *54*, 828−836.
(48) Lash, T. D.; Chandrasekar, P. *J. Am. Chem. Soc.* **1996**, *118*, 8767−8768.
(49) Colby, D. A.; Lash, T. D. *Chem. - Eur. J.* **2002**, *8*, 5397−5402.
(50) Frisch, M. J.; Trucks, G. W.; Schlegel, H. B.; Scuseria, G. E.; Robb, M. A.; Cheeseman, J. R.; Montgomery, J. A., Jr.; Vreven, T.; Kudin, K. N.; Burant, J. C.; et al. *Gaussian 03*, Revision C.02; Gaussian, Inc: Wallingford, CT, 2004.
(51) Wolinski, K.; Hinton, J. F.; Pulay, P. *J. Am. Chem. Soc.* **1990**, *112*, 8251−8260.
(52) Herges, R.; Geuenich, D. *J. Phys. Chem. A* **2001**, *105*, 3214−3220.

DOI: 10.1021/acs.joc.7b00829
J. Org. Chem. 2017, 82, 6680−6688